CrystEngComm

Cite this: *CrystEngComm*, 2011, **13**, 6192

www.rsc.org/crystengcomm

PAPER

Zinc(II) and cadmium(II) coordination polymers mediated by rationally designed symmetrical/asymmetrical *V*-shaped heterocyclic aromatic ligands exhibiting different supramolecular architectures†

Shu-Jun Fu, Li Wang, Tao Tao, Bin Hu, Wei Huang* and Xiao-Zeng You

Received 4th May 2011, Accepted 6th July 2011
DOI: 10.1039/c1ce05516j

Two novel *V*-shaped heterocyclic aromatic ligands, *i.e.*, 3,4-diimidazol-thiophene (**Lsym**, symmetrical) and 3-imidazol-4-pyridinyl-thiophene (**Lasym**, asymmetrical), have been designed and prepared from the carbon–nitrogen and carbon–carbon bond cross-coupling reactions. X-Ray single-crystal structural studies for these ligands and their zinc(II) and cadmium(II) fluorescent coordination polymers reveal that they are formulated as $\{[Zn(\mathbf{Lasym})_2]_3(ClO_4)_6(H_2O)\}_n$ (**1**), $\{[Cd(\mathbf{Lsym})_2Cl_2]\}_n$ (**2**), $\{[Zn(\mathbf{Lsym})_2(CH_3OH)_2](NO_3)_2(CH_3OH)_2\}_n$ (**3**) and $\{[Cd(\mathbf{Lsym})_2(CH_3OH)_2](NO_3)_2(CH_3OH)_2\}_n$ (**4**). The coordination geometry of the metal centers and the molecular conformation of the symmetrical/asymmetrical *V*-shaped ligands **Lsym** and **Lasym**, namely variation of the bite angle θ between the two coordination nitrogen atoms and the central sulfur atom of thiophene ring as well as the dihedral angles between adjacent aromatic rings, play important roles in tuning the different supramolecular architectures of their metal complexes.

Introduction

Thiophenes and their derivatives have been extensively and thoroughly studied in the field of molecular-based materials[1] such as organic and polymeric light emitting diodes[2] and field effect transistors,[3] because they are believed to be ideal functional elements and building blocks in the studies of molecular electronics. On the one hand, the high polarizability of the sulfur atoms in the thiophene rings leads to the stabilization of the conjugated chains.[4] On the other hand, not only are their electronic, optical, and redox properties intriguing, but also their unique self-assembled properties on the solid surface and in the bulk.[5] More importantly, the enormous and attractive potential of structural variations makes possible the fine tuning of opto-electronic properties in a wide range.

Metal coordination polymers (MCPs) on the basis of self-assembly of a variety of metal ions and multi-functional organic ligands have been rapidly developed because of their intriguing molecular topologies and potential applications.[6] In many cases, competing supramolecular interactions give rise to different supramolecular architectures in response to subtle changes of ligand or counter anion. Therefore, rational design and synthesis of extended heterocyclic aromatic systems for constructing novel functional MCPs are very important and have interesting issues among them. However, limited by the tremendous gap between structures and properties, these problems have not been completely solved up till now. From the basic research perspective, thiophene-based heterocyclic aromatic MCPs have internal advantages exhibiting interesting chemical and physical properties, and their fascinating applications could provide opportunities to bridge the gap, where many tunable structures and properties can be achieved before and after the metal-ion complexation.[7]

In our previous work, a series of aromatic rings (for instance, phenyl, imidazole, thiophene and oligothiophene groups) have been successfully introduced to 3,8-dibromo-1,10-phenanthroline and 2,5-dibromothiophene systems by carbon–carbon bond and/or carbon–nitrogen bond cross-coupling reactions.[8] Furthermore, temperature-dependent semiconducting and photoresponsive properties of self-assembled nanocomposite films and nanodevices fabricated from these compounds and their metal complexes have been explored.[9] In view of the relatively fewer investigations on β,β′-thiophene based heterocyclic aromatic derivatives in comparison with α,α′-thiophene ones[1,5] and rare studies on the conjugated materials derived from 3,4-dibromothiophene with metal binding sites,[10] we report herein two new *V*-shaped thiophene-based heterocyclic aromatic bridging ligands (Scheme 1), *i.e.* 3,4-diimidazol-thiophene (**Lsym**, symmetrical) and 3-imidazol-4-pyridinyl-thiophene (**Lasym**, asymmetrical), and their one-dimensional (1D) and two-dimensional (2D) zinc(II) and cadmium(II) polymeric complexes **1–4** with dissimilar supramolecular architectures directed by the

State Key Laboratory of Coordination Chemistry, Nanjing National Laboratory of Microstructures, School of Chemistry and Chemical Engineering, Nanjing University, Nanjing, 210093, P. R. China. E-mail: whuang@nju.edu.cn; Fax: +86-25-83314502; Tel: +86-25-83686526

† Electronic supplementary information (ESI) available: Intermolecular hydrogen bonds in **Lsym**, **L1** and **1–4**, ^1H and ^{13}C NMR spectra of **Lsym** and **Lasym**, π-packing and H-bonding diagrams of **L1**, and simulated and experimental PXRD patterns for MCPs **1–4**. CCDC reference numbers 815007–815012 for **Lsym**, **L1** and **1–4**. For ESI and crystallographic data in CIF or other electronic format, see DOI: 10.1039/c1ce05516j

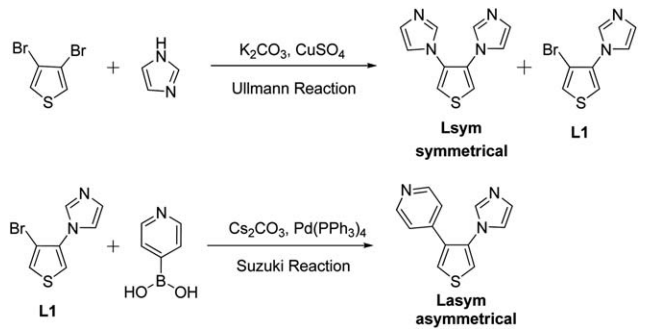

Scheme 1 Schematic illustration of the preparation of compounds **Lsym**, **Lasym** and **L1**.

different symmetries of *V*-shaped ligands **Lsym** and **Lasym** as well as the coordination modes of the metal centers (Scheme 2).

Experimental section

Materials and measurements

All melting points were measured without correction. The reagents of analytical grade were purchased from commercial sources and used without any further purification. Anhydrous solvents were drawn into syringes under a flow of dry argon and directly transferred into the reaction flasks to avoid contamination. Column chromatography was carried out on silica gel (300–400 mesh) and analytical thin-layer chromatography (TLC) was performed on glass plates of silica gel GF-254 with detection by UV. Standard techniques for synthesis were carried out under an argon atmosphere. ^{1}H and ^{13}C NMR spectra were obtained on a Bruker AM-500 NMR spectrometer using TMS ($SiMe_4$) as an internal reference and chloroform-*d* ($CDCl_3$) as the solvent at room temperature. Elemental analyses were measured with a Perkin-Elmer 1400C analyzer. Infrared spectra (4000–400 cm^{-1}) were collected on a Nicolet FT-IR 170X spectrophotometer at 25 °C using KBr plates. Ultraviolet-visible (UV-Vis) spectra were recorded on a Shimadzu UV-3100 double-beam spectrometer using a Pyrex cell with a path length of 10 mm at room temperature. Luminescence spectra were recorded on an F-4600 fluorescence spectrophotometer at room temperature using the same solutions as those for the UV-Vis determination. Electrospray ionization mass spectra (ESI-MS) were recorded on a Finnigan MAT SSQ 710 mass spectrometer in a scan range of 200–2000 amu. Luminescence spectra were recorded on a Hitachi 850 fluorescent spectrophotometer at room temperature. Powder X-ray diffraction (PXRD) measurements were performed on a Philips X'pert MPD Pro X-ray diffractometer using Cu-Kα radiation ($\lambda = 0.15418$ nm), in which the X-ray tube was operated at 40 kV and 40 mA at room temperature.

Caution! Perchlorate salts are potentially explosive and should only be prepared in small quantities; no such problems were encountered in any of the syntheses reported, but ***great care*** must always be exercised.

Syntheses of ligands 4-bromo-3-imidazole thiophene (L1) and 3,4-diimidazole thiophene (Lsym)

Imidazole (6.81 g, 100.0 mmol), 3,4-dibromothiophene (2.42 g, 10.0 mmol), anhydrous $CuSO_4$ (0.08 g, 0.5 mmol), anhydrous K_2CO_3 (3.32 g, 24.0 mmol) and *N*,*N*′-dimethylformamide (50 cm^3) were added to a flask fitted with a magnetic stir bar, a condenser and sealed with an argon balloon. The reaction mixture was stirred at 125 °C for 40 h under the positive pressure of argon. After 3,4-dibromothiophene was completely consumed which could be detected by TLC analysis, the reaction was stopped and the mixture was cooled to room temperature and filtered. After being rinsed with another 50 cm^3 of ethyl acetate, the combined filtrate was then washed with saturated brine (20 cm^3 × 3), dried by anhydrous Na_2SO_4, and concentrated to *ca.* 2 cm^3 by a rotatory evaporator. The residue was purified by careful column chromatography on silica gel eluted with petroleum ether (PE) and then PE/EA (1 : 4). The first yellow solid (**L1**) was obtained in a yield of 0.77 g (33.8%). Mp: 71–72 °C. Elemental anal. calcd. for $C_7H_5BrN_2S$: C, 36.70; H, 2.20; N, 12.23%. Found:

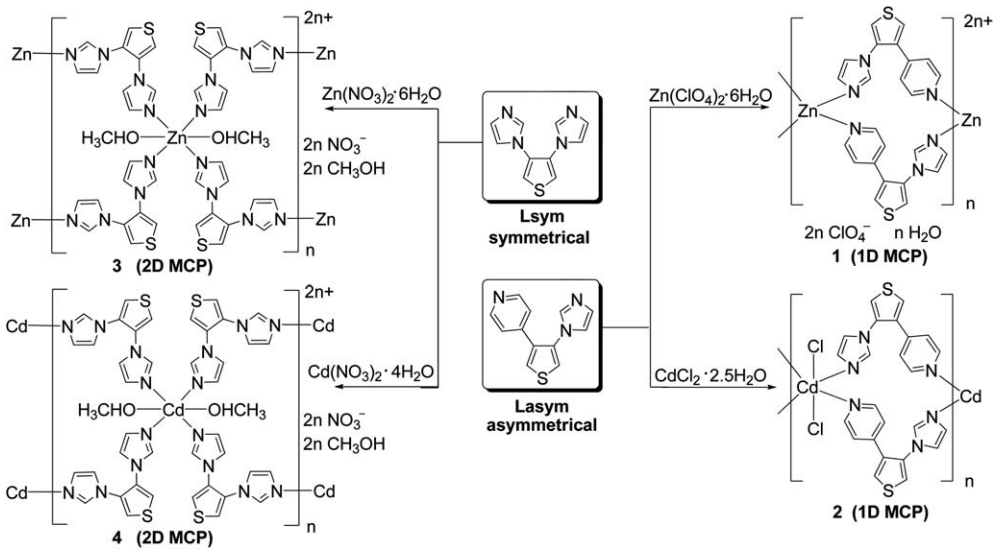

Scheme 2 Schematic illustration of the preparation of metal complexes **1**–**4**.

C, 36.51; H, 2.43; N, 12.34%. Main FT-IR absorptions (KBr pellets, cm^{-1}): 3446 (s), 3108 (m), 2362 (w), 1650 (m), 1537 (s), 1487 (m), 1382 (s), 1330 (m), 1238 (m), 1165 (m), 1060 (s), 897 (s), 831 (s), 726 (s), 659 (s). ^{1}H NMR (500 MHz, $CDCl_3$, 298 K, TMS, ppm) $\delta = 7.74$ (s, 1H, imidazole), 7.42 (d, $J = 3.7$ Hz, 1H, imidazole), 7.33 (d, $J = 3.7$ Hz, 1H, imidazole), 7.21 (s, 1H, thiophene), 7.18 (s, 1H, thiophene). ESI-MS (*m*/*z*): Calcd. for $[C_7H_5BrN_2S]^+$ 229.1, found 229.0. UV-Vis in methanol, $\lambda_{max}/\varepsilon$ (L mol^{-1} cm^{-1}) = 246 (16 200) nm. The second yellow solid (**Lsym**) was obtained in a yield of 1.20 g (55.4%). Mp: 190–192 °C. Elemental anal. calcd. for $C_{10}H_8N_4S$: C, 55.54; H, 3.73; N, 25.91%. Found: C, 55.33; H, 3.92; N, 25.70%. Main FT-IR absorptions (KBr pellets, ν, cm^{-1}): 3105 (m), 3057 (b), 1638 (m), 1556 (s), 1528 (s), 1506 (s), 1486 (s), 1334 (m), 1304 (m), 1269 (m), 1237 (s), 1109 (m), 1088 (m), 1069 (s), 1043 (s), 909 (m), 859 (m), 822 (m). ^{1}H NMR (500 MHz, $CDCl_3$, 298 K, TMS, ppm) $\delta = 7.46$ (d, $J = 9.3$ Hz, 4H, imidazole), 7.12 (s, 2H, imidazole), 6.77 (s, 2H, thiophene). ^{13}C NMR (125 MHz, $CDCl_3$) δ = 136.73, 130.52, 130.40, 120.01, 119.24. ESI-MS, *m*/*z*: Calcd. for $[C_{10}H_9N_4S]^+$ 217.3, found 217.0. UV-Vis in methanol, $\lambda_{max}/\varepsilon$ (L mol^{-1} cm^{-1}) = 207 (42 600), 243 (16 700) nm. Fluorescence emission in methanol, $\lambda_{max} = 394$ nm. The light yellow single crystals of **L1** and **Lsym** suitable for X-ray diffraction determination were grown from their $CHCl_3$ solutions by slow evaporation in air at room temperature.

3-Imidazol-4-pyridinyl-thiophene (Lasym)

Compound **L1** (0.23 g, 1.0 mmol), 4-pyridinyl boronic acid (0.16 g, 1.3 mmol), Cs_2CO_3 (0.56 g, 1.7 mmol), $[Pd(PPh_3)_4]$ (0.04 g), dioxane (20 cm^3) and H_2O (2 cm^3) were added to a flask fitted with a magnetic stir bar, a condenser and sealed with an argon balloon. The reaction mixture was stirred at 98 °C for 48 h under the positive pressure of argon. After compound **L1** was completely consumed, the reaction was stopped and the mixture was cooled to room temperature and filtered. After being rinsed with another 50 cm^3 of CH_2Cl_2, the combined filtrate was washed with saturated brine (10 cm^3 × 3), dried by anhydrous Na_2SO_4, and concentrated to *ca.* 2 cm^3 by a rotatory evaporator. The residue was purified by column chromatography on silica gel eluted with EA. White solid **Lasym** was obtained in a yield of 0.21 g (92.1%). Mp: 189–190 °C. Elemental anal. calcd. for $C_{12}H_9N_3S$: C, 63.41; H, 3.99; N, 18.49%. Found: C, 63.30; H, 3.92; N, 18.61%. Main FT-IR absorptions (KBr pellets, cm^{-1}): 3421 (s), 3064 (m), 1643 (w), 1592 (s), 1413 (m), 1054 (s), 823 (s), 657 (s), 617 (m). ^{1}H NMR (500 MHz, $CDCl_3$) $\delta = 8.54$ (d, $J =$ 5.9 Hz, 2H, pyridine), 7.57 (d, $J = 3.4$ Hz, 1H, imidazole), 7.52 (s, 1H, imidazole), 7.44 (d, $J = 3.4$ Hz, 1H, imidazole), 7.15 (s, 1H, thiophene), 6.95 (d, $J = 6.0$ Hz, 2H, pyridine), 6.88 (s, 1H, thiophene). ^{13}C NMR (125 MHz, $CDCl_3$) δ = 150.33, 140.94, 137.31, 135.08, 133.96, 129.99, 125.96, 121.90, 121.45, 120.37. ESI-MS (*m*/*z*): Calcd. for $[C_{12}H_9N_3S]^+$ 227.3, found 227.0. UV-Vis in methanol, $\lambda_{max}/\varepsilon$ (L mol^{-1} cm^{-1}) = 257 (44 250) nm. Fluorescence emission in methanol, $\lambda_{max} = 393$ nm.

Preparation of the zinc(II) and cadmium(II) coordination polymers 1–4

$\{[Zn(Lasym)_2]_3(ClO_4)_6(H_2O)\}_n$ (1). A mixture of **Lasym** (0.050 g, 0.22 mmol), $Zn(ClO_4)_2 \cdot 6H_2O$ (0.075 g, 0.20 mmol), water (0.5 cm^3) and ethanol (10 cm^3) was frozen and sealed under a vacuum in a thick-walled Pyrex tube, then placed inside an oven at 130 °C for 60 h. Colorless crystals of **1** were obtained in a yield of 0.024 g (38.1%) on the basis of **Lasym**. Elemental anal. calcd. for $C_{72}H_{56}Cl_6N_{18}O_{25}S_6Zn_3$: C, 39.77; H, 2.60; N, 11.59%. Found: C, 39.72; H, 2.55; N, 11.64%. Main FT-IR absorptions (KBr pellets, cm^{-1}): 3419 (m), 3146 (m), 3099 (m), 1619 (s), 1557 (m), 1529 (s), 1428 (w), 1253 (w), 1088 (s), 955 (w), 865 (m), 839 (m), 655 (m), 621 (s), 554(w). UV-Vis in methanol, $\lambda_{max}/\varepsilon$ (L mol^{-1} cm^{-1}) = 207 (17 000) and 257 (9650) nm. Fluorescence emission in methanol, $\lambda_{max} = 408$ nm.

$\{[Cd(Lasym)_2Cl_2]\}_n$ (2). To a stirred solution of $CdCl_2 \cdot 2.5H_2O$ (0.046 g, 0.20 mmol) in CH_3OH (5 cm^3) and CH_3CN (5 cm^3) was added a solution of **Lasym** (0.050 g, 0.22 mmol) in CH_3OH (25 cm^3) and CH_3CN (25 cm^3). The resulting mixture was refluxed for 2 h then cooled to room temperature. White microcrystals of **2** were collected in a yield of 0.078 g (61.1%). Elemental anal. calcd. for $C_{24}H_{18}CdCl_2N_6S_2$: C, 45.19; H, 2.84; N, 13.17%. Found: C, 45.14; H, 2.81; N, 13.22%. Main FT-IR absorptions (KBr pellets, cm^{-1}): 3411 (s), 3098 (m), 3049 (m), 1607 (s), 1553 (w), 1510 (w), 1317 (w), 1111 (m), 1062 (s), 924 (w), 824 (m), 791 (w), 658 (s), 624 (s), 556 (w). UV-Vis in methanol, $\lambda_{max}/\varepsilon$ (L mol^{-1} cm^{-1}) = 207 (24 250) and 257 (13 350) nm. Fluorescence emission in methanol, $\lambda_{max} = 371$ nm.

$\{[Zn(Lsym)_2(CH_3OH)_2](NO_3)_2(CH_3OH)_2\}_n$ (3). To a stirred solution of $Zn(NO_3) \cdot 6H_2O$ (0.058 g, 0.20 mmol) in CH_3OH (5 cm^3) was added a solution of **Lsym** (0.048 g, 0.22 mmol) in CH_3OH (25 cm^3). The resulting mixture was refluxed for 2 h and cooled to room temperature. Colorless crystals of **3** were collected in a yield of 0.089 g (59.2%). Elemental anal. calcd. for $C_{24}H_{32}N_{10}O_{10}S_2Zn$: C, 38.43; H, 4.30; N, 18.67%. Found: C, 38.38; H, 4.26; N, 18.71%. Main FT-IR absorptions (KBr pellets, cm^{-1}): 3419 (m), 3097 (w), 3070 (w), 1635 (w), 1532 (m), 1515 (m), 1373 (s), 1328 (s), 1007 (s), 1082 (w), 954 (w), 820 (w), 766 (w), 647 (w). UV-Vis in methanol, $\lambda_{max}/\varepsilon$ (L mol^{-1} cm^{-1}) = 208 (76 850) and 247 (10 800) nm. Fluorescence emission in methanol, $\lambda_{max} = 421$ nm.

$\{[Cd(Lsym)_2(CH_3OH)_2](NO_3)_2(CH_3OH)_2\}_n$ (4). To a stirred solution of $Cd(NO_3) \cdot 4H_2O$ (0.062 g, 0.20 mmol) in CH_3OH (5 cm^3) was added a solution of **Lsym** (0.048 g, 0.20 mmol) in CH_3OH (25 cm^3). The resulting mixture was refluxed for 2 h and cooled to room temperature. Light yellow microcrystals of **4** were collected in a yield of 0.098 g (61.3%). Elemental anal. calcd. for $C_{24}H_{32}CdN_{10}O_{10}S_2$: C, 36.16; H, 4.05; N, 17.57%. Found: C, 36.11; H, 4.01; N, 17.61%. Main FT-IR absorptions (KBr pellets, cm^{-1}): 3416 (m), 3113 (m), 1640 (w), 1571 (w), 1539 (m), 1526 (m), 1400 (s), 1310 (s), 1098 (m), 1069 (m), 1042 (m), 931 (w), 822 (w), 744 (w), 652 (m). UV-Vis in methanol, $\lambda_{max}/\varepsilon$ (L mol^{-1} cm^{-1}) = 207 (39 950) and 245 (10 400) nm. Fluorescence emission in methanol, $\lambda_{max} = 423$ nm.

Crystallography

All single-crystal samples of **Lsym**, **L1** and **1–4** were covered with glue and mounted on glass fibers for data collection with Mo-Kα radiation (λ = 0.71073 Å) on a Bruker SMART 1 K

diffractometer equipped with a CCD camera. Data collection was performed by using the SMART program and cell refinement and data reduction were made with the SAINT program.[11] The crystal systems were determined by Laue symmetry and the space groups were assigned on the basis of systematic absences using XPREP, and then the structures were solved by direct methods and refined by the least-squares method on F^2_{obs} by using the SHELXTL-PC software package.[12] All non-H atoms were anisotropically refined and all hydrogen atoms were inserted in the calculated positions, assigned fixed isotropic thermal parameters and allowed to ride on their respective parent atoms. In the case of zinc(II) complex **1**, the unique water oxygen O5 lies at a site with imposed 3_2 symmetry, so it is refined isotropically with no allowance for water H atoms. All calculations were made on a PC computer and molecular graphics were drawn by using XSHELL, MERCURY and DIAMOND software. The summary of the data collection and refinement for **Lsym**, **L1** and **1–4** is given in Table 1, whereas the selected bond lengths and angles are listed in Table 2.

Results and discussion

Syntheses and spectral characterizations

3,4-Diimidazol-thiophene (**Lsym**) and 4-bromo-3-imidazol-thiophene (**L1**) were prepared *via* the carbon–nitrogen bond cross-coupling reaction between 3,4-dibromothiophene and imidazole using Ullmann condensation methods,[13] while 3-imidazol-4-pyridinyl-thiophene (**Lasym**) was synthesized *via* the carbon–carbon bond cross-coupling reaction between **L1** and 4-pyridinyl-boronic acid using Suzuki reactions[14] due to the low reaction activity of the pyridine coupling component (Scheme 1). As can ben seen in Fig. SI1–3 in the ESI,† the formation of compounds **L1**, **Lsym** and **Lasym** has been clearly verified by their ^{1}H and ^{13}C NMR spectra. MCPs **1–4** can be yielded by the treatment of different metal salts with the symmetrical/asymmetrical *V*-shaped heterocyclic aromatic ligands **Lsym** and **Lasym** in the process of metal-ion complexation and the experimental results are easy to be reproduced. Considering that ligand **Lsym** crystallizes in a non-centrosymmetric space group, the non-linear optical properties of **Lsym** were investigated according to the principles proposed by Kurtz and Perry.[15] The strength of the second harmonic generation (SHG) efficiency of **Lsym** was tested by measuring the microcrystalline powder samples, and our preliminary experimental results show that **Lsym** is SHG-active and the SHG efficiency is approximately 0.6 times that of urea.

UV-Vis absorption spectra of free *V*-shaped ligands **Lsym** and **Lasym** as well as their metal complexes **1–4** in methanol are illustrated in the inset of Fig. 1. Compared with the absorptions of ligand **Lsym**, the π–π* transition between the heterocyclic aromatic rings of ligand **Lasym** shows a bathochromic shift of 14 nm from 243 to 257 nm. In contrast, subtle changes are observed around this wavelength band for their zinc(II) and cadmium(II) coordination polymers due to the absence of d–d transitions and metal ligand charge transitions.

Moreover, two ligands and their MCPs **1–4** are found to be fluorescence active because of their rigid molecular structures

Table 1 Crystal and refinement data for compounds **Lsym**, **L1** and **1–4**

Compound	**Lsym**	**L1**	**1**	**2**	**3**	**4**
Empirical formula	$C_{10}H_8N_4S$	$C_7H_5BrN_2S$	$C_{72}H_{54}Cl_6N_{18}O_{25}S_6Zn_3$	$C_{24}H_{18}CdCl_2N_6S_2$	$C_{24}H_{32}N_{10}O_{10}S_2Zn$	$C_{24}H_{32}CdN_{10}O_{10}S_2$
Formula weight	216.27	229.10	2172.50	637.86	750.13	797.15
Cryst. size/mm	0.10 × 0.14 × 0.18	0.12 × 0.10 × 0.15	0.11 × 0.11 × 0.10	0.12 × 0.11 × 0.10	0.11 × 0.12 × 0.12	0.10 × 0.11 × 0.12
Cryst. syst.	Trigonal	Triclinic	Trigonal	Monoclinic	Monoclinic	Monoclinic
Space group	$P3_221$	$P\bar{1}$	$R\bar{3}c$	$P2_1/c$	$P2_1/c$	$P2_1/c$
a/Å	7.314(1)	6.969(3)	23.836(1)	8.184(1)	9.036(1)	9.089(1)
b/Å	7.314(1)	7.073(3)	23.836(1)	9.697(1)	15.987(2)	16.377(2)
c/Å	16.496(2)	9.075(4)	26.589(2)	15.710(1)	12.543(2)	12.680(1)
α (°)	90.00	92.827(5)	90.00	90.00	90.00	90.00
β (°)	90.00	106.248(4)	90.00	104.448(1)	116.040(1)	116.015(1)
γ (°)	120.00	99.958(6)	120.00	90.00	90.00	90.00
V/Å^3	764.14(11)	420.7(3)	13 083.2(12)	1207.33(11)	1627.9(3)	1696.1(3)
Z/D_c/g cm^{-3}	3/1.410	2/1.808	6/1.656	2/1.755	2/1.530	2/1.561
F(000)	336	224	6612	636	776	812
μ/mm^{-1}	0.287	5.065	1.232	1.326	0.951	0.833
Max/min transmission	0.9719/0.9502	0.6313/0.6313	0.8867/0.8764	0.8788/0.8571	0.9026/0.8944	0.9214/0.9067
h_{min}/h_{max}	−9/9	−7/8	−28/27	−9/7	−10/10	−9/10
k_{min}/k_{max}	−9/9	−8/7	−18/28	−11/10	−19/11	−15/19
l_{min}/l_{max}	−21/17	−10/10	−31/31	−18/17	−14/14	−14/14
Flack	−0.03(10)					
Data/parameters	1243/69	1450/100	2566/196	2121/160	2847/214	2973/214
Final *R* indices [$I > 2\sigma(I)$][a]	$R_1 = 0.0322$, wR_2 = 0.0855	$R_1 = 0.0726$, wR_2 = 0.1721	$R_1 = 0.0407$, wR_2 = 0.1004	$R_1 = 0.0215$, wR_2 = 0.0473	$R_1 = 0.0288$, wR_2 = 0.0672	$R_1 = 0.0312$, wR_2 = 0.0529
R indices (all data)	$R_1 = 0.0334$, wR_2 = 0.0871	$R_1 = 0.0839$, wR_2 = 0.1822	$R_1 = 0.0647$, wR_2 = 0.1071	$R_1 = 0.0268$, wR_2 = 0.0490	$R_1 = 0.0376$, wR_2 = 0.0698	$R_1 = 0.0478$, wR_2 = 0.0561
S	1.047	0.904	0.935	0.927	0.953	0.845
Max./min. Δ*ρ*/e Å^{-3}	0.15/−0.21	1.05/−1.41	0.42/−0.31	0.24/−0.30	0.28/−0.22	0.37/−0.28

[a] $R1 = \Sigma||Fo| - |Fc||/\Sigma|Fo|$, $wR2 = [\Sigma[w(Fo^2 - Fc^2)^2]/\Sigma w(Fo^2)^2]^{1/2}$.

Table 2 Selected bond distances (Å) and angles (°) for compounds **Lsym**, **L1** and **1–4**[a]

Bond distances		Bond angles	
Lsym			
S1–C1	1.705(2)	C1–S1–C1[a]	92.5(1)
N1–C2	1.421(2)	C2–N1–C3	126.3(1)
N1–C3	1.357(2)	C2–N1–C5	126.8(1)
N1–C5	1.370(2)	C3–N1–C5	106.3(1)
N2–C3	1.304(3)	C3–N2–C4	105.1(2)
N2–C4	1.370(2)	S1–C1–C2	111.4(1)
L1			
N1–C2	1.421(8)	C1–S2–C4	92.1(4)
N1–C5	1.357(8)	C2–N1–C7	126.9(5)
N1–C7	1.361(9)	C2–N1–C5	126.4(5)
N2–C5	1.317(8)	C5–N1–C7	106.6(5)
N2–C6	1.366(9)	C5–N2–C6	105.3(6)
S2–C1	1.706(7)	N1–C5–N2	111.4(6)
S2–C4	1.680(8)	Br1–C3–C2	123.6(5)
Br1–C3	1.878(7)	Br1–C3–C4	124.3(6)
1			
Zn1–N1	2.042(3)	N1–Zn1–N3[b]	115.0(1)
Zn1–N3[b]	1.974(3)	N1–Zn1–N3[c]	99.5(1)
Zn1–N3[c]	1.974(3)	N1–Zn1–N1[d]	107.7(2)
Zn1–N1[d]	2.042(3)	N3[b]–Zn1–N3[c]	120.3(2)
2			
Cd1–Cl1	2.592(1)	Cl1–Cd1–N3	92.4(1)
Cd1–N3	2.391(2)	Cl1–Cd1–N1[e]	88.9(1)
Cd1–N1[e]	2.382(2)	Cl1–Cd1–N1[f]	91.1(1)
Cd1–N1[f]	2.382(2)	Cl1–Cd1–N3[g]	87.6(1)
Cd1–Cl1[g]	2.592(1)	N1[e]–Cd1–N3	88.3(1)
Cd1–N3[g]	2.391(2)	N1[f]–Cd1–N3	91.7(1)
		Cl1[g]–Cd1–N1[e]	91.1(1)
		N1e–Cd1–N3[g]	91.7(1)
		Cl1[g]–Cd1–N1[f]	88.9(1)
		Cl1[g]–Cd1–N3[g]	92.4(1)
3			
Zn1–O1	2.171(2)	O1–Zn1–N1	91.8(1)
Zn1–N1	2.170(2)	O1–Zn1–N4[j]	91.4(1)
Zn1–N4[j]	2.125(2)	O1–Zn1–N1[k]	88.2(1)
Zn1–O1[k]	2.171(2)	O1–Zn1–N4[l]	88.6(1)
Zn1–N1[k]	2.170(2)	O1[k]–Zn1–N1	88.2(1)
Zn1–N4[l]	2.125(2)	O1[k]–Zn1–N4[j]	88.6(1)
		N1–Zn1–N4[l]	89.9(1)
		N1–Zn1–N4[j]	90.1(1)
4			
Cd1–O1	2.345(3)	O1–Cd1–N1	92.4(1)
Cd1–N1	2.328(2)	O1–Cd1–N4[m]	90.8(1)
Cd1–N4[m]	2.282(2)	O1–Cd1–N1[n]	87.6(1)
Cd1–O1[n]	2.345(3)	O1–Cd1–N4[o]	89.2(1)
Cd1–N1[n]	2.328(2)	O1[n]–Cd1–N1	87.6(1)
Cd1–N4[o]	2.282(2)	N1–Cd1–N4[m]	90.5(1)
		N1–Cd1–N4[o]	89.5(1)

[a] Symmetry codes: [a]: $1 + x - y, 2 - y, 1/3 - z$; [b]: $4/3 - y, -1/3 + x - y, -1/3 + z$; [c]: $1/3 + x - y, 2/3 - y, 1/6 - z$; [d]: $2/3 + y, -2/3 + x, -1/6 - z$; [e]: $x, 1 + y, z$; [f]: $2 - x, -y, -z$; [g]: $2 - x, 1 - y, -z$; [j]: $1 - x, -1/2 + y, 3/2 - z$; [k]: $1 - x, -y, 2 - z$; [l]: $x, 1/2 - y, 1/2 + z$; [m]: $1 - x, -1/2 + y, 1/2 - z$; [n]: $1 - x, -y, -z$; [o]: $x, 1/2 - y, -1/2 + z$.

and full $3d^{10}$ electronic structures of Zn(II) and Cd(II) centers, and their fluorescence emission spectra in methanol are shown in Fig. 1 where the same solutions for UV-Vis spectral determination are used. Compared with the fluorescence emission peak at 393 nm for ligand **Lasym**, complex **1** shows a bathochromic shift to 408 nm, while complex **2** exhibits a hypsochromic shift to 371 nm. The variations of molecular conformation of ligand **Lasym** in **1** and **2** (the dihedral angles between adjacent aromatic heterocycles) after metal-ion complexation and coordination

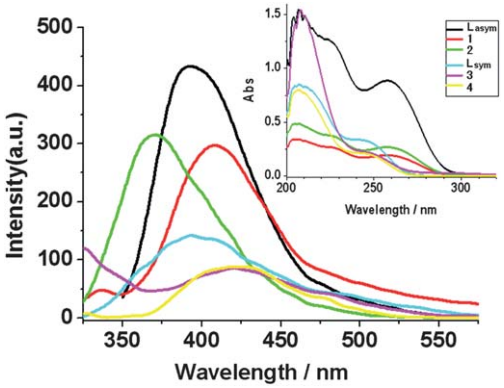

Fig. 1 Fluorescence emission and UV-Vis absorption spectra (inset) of ligands **Lsym** and **Lasym** as well as their metal complexes **1–4** in their methanol solutions.

geometry of Zn(II) and Cd(II) centers (tetrahedron *versus* octahedron) are believed to contribute greatly to the alteration of fluorescence emission. In contrast, complexes **3** and **4** exhibit similar fluorescence emissions at 421 and 423 nm, respectively, because of their isomorphous structures.

Additionally, the pure phases of all four MCPs **1–4** in this work have been confirmed by PXRD patterns, as illustrated in Fig. SI4–7 in the ESI.†

Structural descriptions of Lsym and L1. The molecular structures of **Lsym** and **L1** with the atom-numbering schemes are shown in Fig. 2a and Fig. 2b, respectively. X-Ray diffraction studies of **Lsym** indicate that it crystallizes in the trigonal non-centrosymmetric space group $P3_221$ with a reasonable Flack parameter of −0.03(10) and the molecule lies about a twofold axis with the S1 atom on the twofold axis. The two side imidazole rings are not coplanar to the central thiophene ring. Instead, they are staggered at each side of the thiophene plane with the same dihedral angle of 66.8(2)°. The two nitrogen atoms of imidazole rings point in opposite directions to the central thiophene plane and the separation between them is 6.302(2) Å. There are weak C–H···N hydrogen bonding interactions (Table SI1, ESI†) between adjacent molecules forming continuous 14-membered hydrogen-bonded rings, as can be seen in Fig. 3.

X-Ray diffraction studies of intermediate **L1** indicate that it crystallizes in the triclinic space group $P\bar{1}$ and the dihedral angle

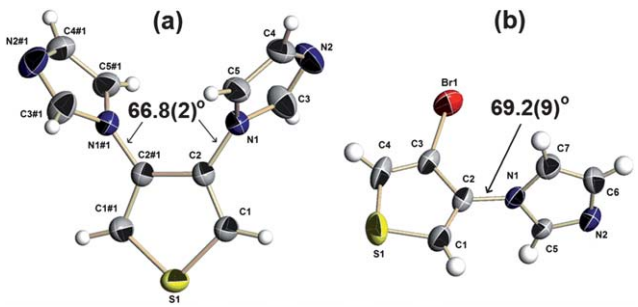

Fig. 2 ORTEP drawings of **Lsym** (**a**) and **L1** (**b**) with the atom-numbering schemes. Displacement ellipsoids are drawn at the 30% probability level. Symmetry codes: #1: $1 + x - y, 2 - y, 1/3 - z$.

between the imidazole ring and the thiophene ring is 69.2(9)°. In the crystal packing of **L1**, π–π stacking interactions are found between neighboring thiophene rings with the centroid-to-centroid separation of 3.899(8) Å. Furthermore, there are weak C–H···N hydrogen bonds between adjacent imidazole rings constituting six-membered $C_2N_2H_2$ hydrogen bonding rings (Fig. SI8 in the ESI†).

Structural description of $\{[Zn(Lasym)_2]_3(ClO_4)_6(H_2O)\}_n$ (1). The cationic structure of **1** with the atom-numbering scheme is shown in Fig. 4a where the Zn1 ion lies on a twofold axis. Every Zn(II) ion is four-coordinated by four nitrogen atoms from two imidazole rings and two pyridine rings of four different asymmetric **Lasym** ligands, and the coordination geometry of the Zn(II) center is a slightly distorted tetrahedron with a mean Zn–N bond length of 2.008(3) Å. In this case, the dihedral angle between the pyridine ring and the thiophene ring is 42.6(6)°, while that between the imidazole ring and the thiophene ring is 47.1(4)°. Each **Lasym** acts as a bidentate bridging ligand where the two nitrogen atoms of the imidazole and pyridine rings point in different directions relative to the central thiophene unit. The distances of *a* and *b* defined in Scheme 3 are 6.751(5) and 5.920(5) Å. The bite angle θ between the two coordination nitrogen atoms and the central sulfur atom of the thiophene ring is 59.6(3)°, and the coordination angle of ∠Zn1S1Zn1#1 (#1 = 1/3 + *x* − *y*, 2/3 − *y*, 1/6 − *z*) is 65.1(3)°.

As depicted in Fig. 5, a 1D polymeric chain is constructed in **1** where one Zn(II) ion and two asymmetric *V*-shaped **Lasym** ligands are alternately connected with a Zn–Zn separation of 8.888(5) Å. Moreover, interchain C–H···O hydrogen bonding interactions are present (Table SI1, ESI†), cooperatively stabilizing the neighboring 1D double-strand helixes.

Structural description of $\{[Cd(Lasym)_2Cl_2]\}_n$ (2). As shown in Fig. 4b, the Cd1 ion lies on an inversion centre and each Cd(II) ion is six-coordinated by four nitrogen atoms from two imidazole rings and two pyridine rings in four different **Lasym** ligands and two chloride counterions in the apical positions. The mean Cd–N bond length is 2.387(2) Å, while the Cd–Cl bond length is a little longer (2.592(1) Å). So the coordination geometry for the central Cd(II) ion is elongated octahedral. All the bond lengths in cadmium(II) complex **2** are longer than those in zinc(II) complex **1** mainly due to the larger ionic radius of the Cd(II) ion. Similar to **1**, every **Lasym** acts as a bidentate bridging ligand linking neighboring Cd(II) ions into a 1D coordination polymer where

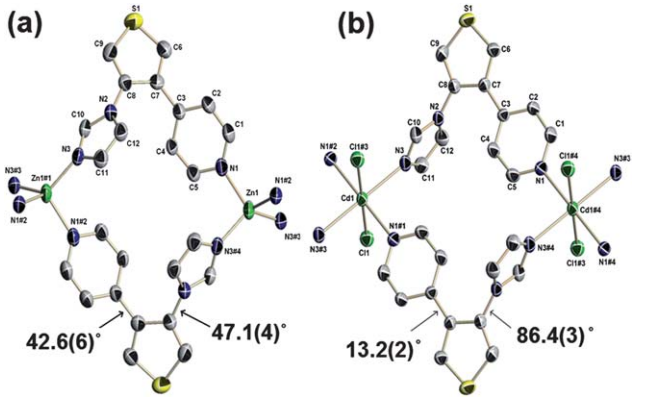

Fig. 4 ORTEP drawing of the cations of **1** (**a**) and **2** (**b**) with the atom-numbering scheme. Displacement ellipsoids are drawn at the 30% probability level. Anions and the H atoms are omitted for clarity. Symmetry codes: (a) #1: 1/3 + *x* − *y*, 2/3 − *y*, 1/6 − *z*; #2: 2/3 + *y*, −2/3 + *x*, −1/6 − *z*; #3: 4/3 − *y*, −1/3 + *x* − *y*, −1/3 + *z*; #4: 1/3 + *x* − *y*, 2/3 − *y*, 1/6 − *z*; (b) #1: *x*, 1 + *y*, *z*; #2: 2 − *x*, −*y*, −*z*; #3: 2 − *x*, 1 − *y*, −*z*; #4: *x*, −1 + *y*, *z*.

the two nitrogen atoms of the imidazole and pyridine rings point in different directions relative to the central thiophene unit. In this 1D chain, one Cd(II) ion and two asymmetric *V*-shaped **Lasym** ligands are alternately connected with a larger Cd–Cd distance of 9.697(2) Å (Fig. 6).

It is suggested that the formation of helical and non-helical structures in **1** and **2** originates from differences in the coordination geometry of the metal centers as well as the molecular conformation of the asymmetric *V*-shaped ligand **Lasym**. With regard to ligand **Lasym** in **2**, the dihedral angle between the pyridine ring and the thiophene ring is 13.2(2)°, while that between the imidazole ring and the thiophene ring is 86.4(3)°. The distances of *a* and *b* are 6.713(3) and 5.991(3) Å, respectively, and the θ angle is 60.4(2)°. The coordination angle of ∠Cd1S1Cd1#4 (#4 = *x*, −1 + *y*, *z*) is 68.8(2)°. In addition, weak interchain C–H···N and C–H···Cl hydrogen bonds (Table SI1, ESI†) are present in **2**, cooperatively stabilizing the neighboring 1D chains and the whole structure.

Structural description of $\{[Zn(Lsym)_2(CH_3OH)_2](NO_3)_2(CH_3OH)_2\}_n$ (3) and $\{[Cd(Lsym)_2(CH_3OH)_2](NO_3)_2(CH_3OH)_2\}_n$ (4). The molecular structures of **3** and **4** with the atom-numbering schemes are shown in Fig. 7a and Fig. 7b, respectively, and the central zinc(II) and cadmium(II) atoms lie on

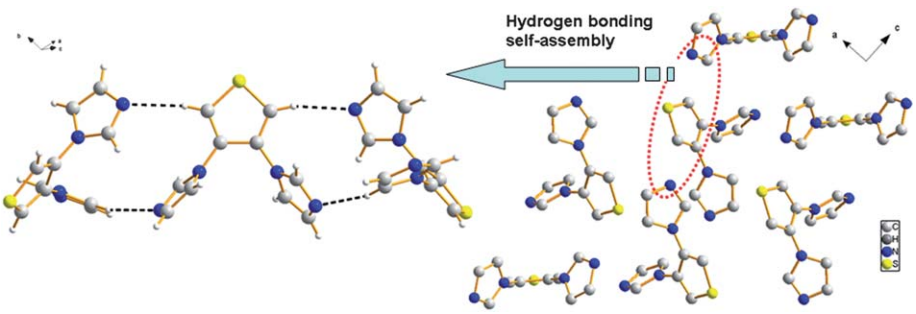

Fig. 3 Perspective view of the hydrogen bonding self-assembly in **Lsym**.

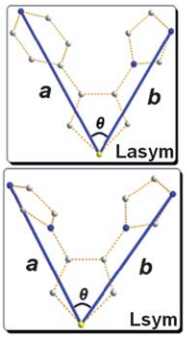

complexes	distances / Å		angle θ / °	architectures
	a	*b*		
$\{[Zn(Lasym)_2]_3(ClO_4)_6(H_2O)\}_n$ (1)	6.751(5)	5.920(5)	59.6(3)	*1D chain*
$\{[Cd(Lasym)_2Cl_2]\}_n$ (2)	6.713(3)	5.991(3)	60.4(2)	*1D chain*
$\{[Zn(Lsym)_2(CH_3OH)_2](NO_3)_2(CH_3OH)_2\}_n$ (3)	5.927(3)	5.890(3)	64.7(2)	*2D network*
$\{[Cd(Lsym)_2(CH_3OH)_2](NO_3)_2(CH_3OH)_2\}_n$ (4)	5.930(5)	5.906(5)	64.1(3)	*2D network*

Scheme 3 Schematic illustration of rationally designed symmetrical/asymmetrical *V*-shaped heterocyclic aromatic ligands.

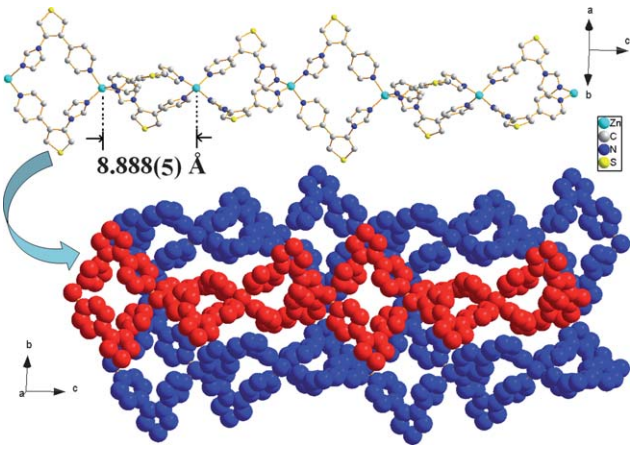

Fig. 5 Perspective view of the 1D chain in the crystal packing of **1**.

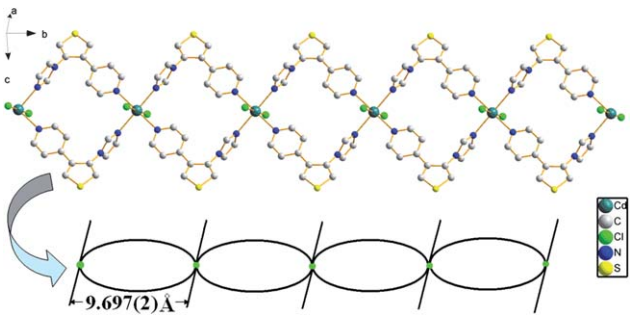

Fig. 6 Perspective view of the 1D chain in the crystal packing of **2**.

inversion centres. These two complexes are nicely isomorphous not merely isostructural, where different divalent cations are present (Zn(II) in **3** and Cd(II) in **4**). Every metal center in **3** and **4** is six-coordinated by four nitrogen atoms of imidazole rings from four different **Lsym** ligands and two oxygen atoms from two solvent methanol molecules. The coordination geometry of the central metal ion is slightly distorted octahedral with the mean coordinative bond lengths of 2.155(2) Å in **3** and 2.318(2) Å in **4** due to the dissimilar ionic radii of Zn(II) and Cd(II) centers. The two nitrogen atoms of the imidazole rings of *V*-shaped ligand **Lsym** point in opposite directions to the central thiophene plane and the separations between them are 6.326(2) Å in **3** and 6.283(2) Å in **4**, which are also different from that in ligand **Lasym** (6.302(2) Å). Every **Lsym** acts as a bidentate bridging ligand linking contiguous two metal ions into 2D coordination networks (Fig. 8), which are different from the 1D coordination polymers in **1** and **2**.

There are continuous rhombus-shaped tetranuclear (M**Lsym**)$_4$ macrocyclic units in the 2D frameworks of **3** and **4** where four thiophene rings of **Lsym** are divided into two groups (Fig. 8). Two facing ones are in the inner opposite sides of the rhombus, while the other pair points to the outer sides of the rhombus. The side lengths of the two rhombuses in **3** and **4** are 10.160(2) and 10.356(2) Å, and the included angles of the two rhombuses are 76.2(1) and 75.5(1)°, respectively. As for the molecular conformation of **Lsym** in MCPs **3** and **4**, the dihedral angles between the imidazole and thiophene rings are 53.9(3) and 59.4(2)° in **3** and 56.0(5) and 57.2(4)° in **4**. The distances of *a* and *b* are 5.927(3) and 5.890(3) Å in **3** and 5.930(5) and 5.906(3) Å in **4**. The *θ* angle and the coordination angle of ∠Zn1S1Zn1#1 (#1 = 1 − *x*, −1/2 + *y*, 3/2 − *z*) in **3** are 64.7(2) and 82.7(2)°, while those in **4** are 64.1 (3) and 82.7(3)°, respectively.

In comparison with α,α′-thiophene based heterocyclic aromatic derivatives generally in the linear configuration, β,β′-thiophene ones preferably adopt the *V*-shaped configuration. As a result, their MCPs exhibit different supramolecular architectures, which are also related to the type of metal centers. In addition, compared with symmetrical *V*-shaped ligands, asymmetrical ones in this work show additional alterations in forming their MCPs. It is also known that anionic and solvent effects influence the architectures of resultant MCPs, especially for

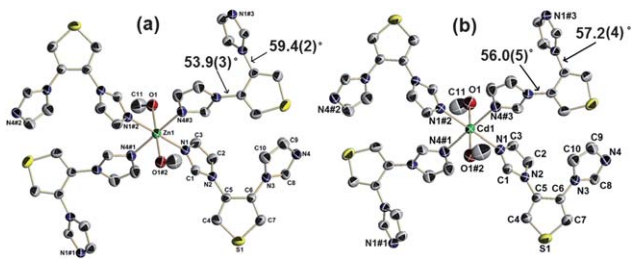

Fig. 7 ORTEP drawing of the cations of **3** (**a**) and **4** (**b**) with the atom-numbering schemes. Displacement ellipsoids are drawn at the 30% probability level. Anions, solvent methanol molecules and the H atoms are omitted for clarity. Symmetry codes: (a) #1: 1 − *x*, −1/2 + *y*, 3/2 − *z*; #2: 1 − *x*, −*y*, 2 − *z*; #3: *x*, 1/2 − *y*,1/2 + *z*; (b) #1: 1 − *x*, −1/2 + *y*, 1/2 − *z*; #2: 1 − *x*, −*y*, −*z*; #3: *x*, 1/2 − *y*, −1/2 + *z*.

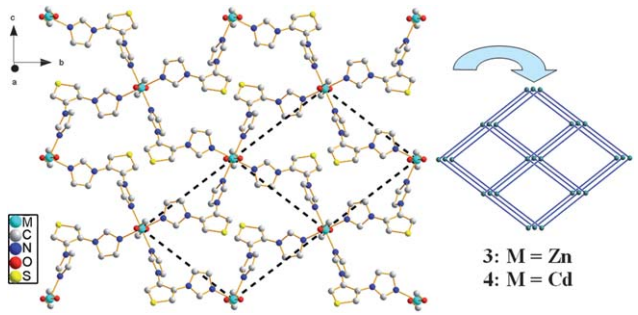

Fig. 8 Perspective view of the 2D network in the crystal packing of **3** and **4**.

those bearing coordination abilities such as Cl^-, NO_3^-, CH_3COO^-, CH_3OH, EtOH and so on. Further investigations are underway on the design and construction of new α,α′-thiophene and β,β′-thiophene based heterocyclic aromatic compounds having interesting optoelectronic properties.

Conclusion

In summary, we have designed and synthesized two novel *V*-shaped symmetrical and asymmetrical ligands **Lsym** and **Lasym**, which are prepared from carbon–carbon and carbon–nitrogen bond cross-coupling reactions from 3,4-dibromothiophene, for the study on thiophene-based heterocyclic aromatic ligand controlled and anion directed MCPs. As a result, two pairs of zinc(II) and cadmium(II) fluorescent coordination polymers **1–4** have been obtained with different coordination modes and supramolecular architectures (1D 3_1 helix in **1**, 1D non-helical chain in **2** and 2D networks in **3** and **4**), where the *V*-shaped heterocyclic aromatic ligands **Lsym** and **Lasym** show different molecular conformations evidenced by the alteration of θ angle and dihedral angles between aromatic rings and the distances of *a* and *b*. It is suggested that the coordination modes of metal centers, the molecular conformation of heterocyclic aromatic ligands **Lsym** and **Lasym**, and the influences of counterions play important roles in dominating the final architectures of MCPs.

Acknowledgements

We acknowledge the Major State Basic Research Development Program (Nos. 2011CB933300, 2007CB925101 and 2011CB808704), the National Natural Science Foundation of China (Nos. 20871065 and 21021062) and the Jiangsu Province Department of Science and Technology (No. BK2009226) for financial aids.

References

1 (*a*) J. Roncali, *Chem. Rev.*, 1997, **97**, 173; (*b*) D. Fichou, *Handbook of Oligo- and Polythiophenes*, Wiley-VCH, Weinheim, Germany 1999; (*c*) R. L. Carroll and C. B. Gorman, *Angew. Chem., Int. Ed.*, 2002, **41**, 4378; (*d*) Y. J. Cheng, S. H. Yang and C. S. Hu, *Chem. Rev.*, 2009, **109**, 5868; (*e*) J. W. Chen and Y. Cao, *Acc. Chem. Res.*, 2009, **42**, 1709; (*f*) W. Wu, Y. Liu and D. Zhu, *Chem. Soc. Rev.*, 2010, **39**, 1489.

2 Selected examples: (*a*) Q. Fang, B. Xu, B. Jiang, H. Fu, X. Chen and A. Cao, *Chem. Commun.*, 2005, 1788; (*b*) C. Du, S. Ye, J. Chen, Y. Guo, Y. Liu, K. Lu, Y. Liu, T. Qi, X. Gao, Z. Shuai and G. Yu, *Chem.–Eur. J.*, 2009, **15**, 8275; (*c*) S. Hamwi, J. Meyer, M. Kroeger, T. Winkler, M. Witte, T. Riedl, A. Kahn and W. Kowalsky, *Adv. Funct. Mater.*, 2010, **20**, 1762.

3 Selected examples: (*a*) M. H. Yoon, A. Facchetti, C. E. Stern and T. J. Marks, *J. Am. Chem. Soc.*, 2006, **128**, 5792; (*b*) Y. Jung, R. J. Kline, D. A. Fischer, E. K. Lin, M. Heeney, I. McCulloch and D. M. DeLongchamp, *Adv. Funct. Mater.*, 2008, **18**, 742; (*c*) D. H. Kim, B. L. Lee, H. Moon, H. M. Kang, E. J. Jeong, J. I. Park, K. M. Han, S. Lee, B. W. Yoo, B. W. Koo, J. Y. Kim, W. H. Lee, K. Cho, H. A. Becerril and Z. Bao, *J. Am. Chem. Soc.*, 2009, **131**, 6124.

4 K. Mullen, G. Wegner, *Electronic Materials: The Oligomer Approach*, Wiley-VCH, Weinheim, 1998.

5 A. Mishra, C. Q. Ma and P. Bauerle, *Chem. Rev.*, 2009, **109**, 1141.

6 (*a*) B. Moulton and M. J. Zaworotko, *Chem. Rev.*, 2001, **101**, 1629; (*b*) A. Erxleben, *Coord. Chem. Rev.*, 2003, **246**, 203; (*c*) S. L. James, *Chem. Soc. Rev.*, 2003, **32**, 276; (*d*) C. Y. Li, C. S. Liu, J. R. Li and X. H. Bu, *Cryst. Growth Des.*, 2007, **7**, 286; (*e*) Y. Z. Zheng, M. L. Tong, W. Xue, W. X. Zhang, X. M. Chen, F. Grandjean and G. J. Long, *Angew. Chem., Int. Ed.*, 2007, **46**, 6076; (*f*) H. Zhao, Q. Ye, Z. R. Qu, D. W. Fu, R. G. Xiong, S. D. Huang and P. W. H. Chan, *Chem.–Eur. J.*, 2008, **14**, 1164; (*g*) B. W. Hu, J. P. Zhao, J. Tao, X. J. Sun, Q. Yang, X. F. Zhang and X. H. Bu, *Cryst. Growth Des.*, 2010, **10**, 2829; (*h*) J. P. Zhao, B. W. Hu, X. F. Zhang, Q. Yang, M. S. El Fallah, J. Ribas and X. H. Bu, *Inorg. Chem.*, 2010, **49**, 11325.

7 (*a*) K. Araki, H. Endo, G. Masuda and T. Ogawa, *Chem.–Eur. J.*, 2004, **10**, 3331; (*b*) H. Suzuki, T. Kanbara and T. Yamamoto, *Inorg. Chim. Acta*, 2004, **357**, 4335.

8 (*a*) W. Huang, G. Masuda, S. Maeda, H. Tanaka, T. Hino and T. Ogawa, *Inorg. Chem.*, 2008, **47**, 468; (*b*) L. Wang, W. You, W. Huang, C. Wang and X. Z. You, *Inorg. Chem.*, 2009, **48**, 4295; (*c*) W. Huang, L. Wang, H. Tanaka and T. Ogawa, *Eur. J. Inorg. Chem.*, 2009, 1321; (*d*) B. Hu, F. Xu, S. J. Fu, T. Tao, Y. N. Wang and W. Huang, *Inorg. Chim. Acta*, 2010, **363**, 1348; (*e*) L. Wang, T. Tao, S. J. Fu, C. Wang, W. Huang and X. Z. You, *CrystEngComm*, 2011, **13**, 747; (*f*) B. Hu, S. J. Fu, F. Xu, T. Tao, H. Y. Zhu, K. S. Cao, W. Huang and X. Z. You, *J. Org. Chem.*, 2011, **76**, 4444.

9 (*a*) W. Huang, G. Masuda, S. Maeda and H. Tanaka, *Chem.–Eur. J.*, 2006, **12**, 607; (*b*) W. Huang, H. Tanaka and T. Ogawa, *J. Phys. Chem. C*, 2008, **112**, 11513; (*c*) W. Huang, H. Tanaka, T. Ogawa and X. Z. You, *Adv. Mater.*, 2010, **22**, 2753.

10 (*a*) A. M. Mohamed, *Synth. Commun.*, 2003, **33**, 153; (*b*) A. S. Balkis, A. M. Mohammed, E. M. Ahmed and E. M. Hilmy, *J. Heterocycl. Chem.*, 2003, **40**, 171; (*c*) A. S. Balkis, E. M. Ahmed and E. M. Hilmy, *J. Heterocycl. Chem.*, 2005, **42**, 483; (*d*) R. A. Altman, E. D. Koval and S. L. Buchwald, *J. Org. Chem.*, 2007, **72**, 6190.

11 *SMART and SAINT, Area Detector Control and Integration Software*, Siemens Analytical X-ray Systems Inc., Madison, WI, 2000.

12 G. M. Sheldrick, *SHELXTL, version 6.10*, Siemens Industrial Automation, Madison, WI, 2000.

13 (*a*) P. E. Fanta, *Synthesis*, 1974, 1; (*b*) J. Lindley, *Tetrahedron*, 1980, **40**, 1433; (*c*) J. F. Hartwig, *Angew. Chem., Int. Ed.*, 1998, **37**, 2046; (*d*) H. B. Goodbrand and N. X. Hu, *J. Org. Chem.*, 1999, **64**, 670.

14 (*a*) J. K. Stille, *Pure Appl. Chem.*, 1985, **57**, 1771; (*b*) N. Miyaura and A. Suzuki, *Chem. Rev.*, 1995, **95**, 2457; (*c*) E. Negishi, *Handbook of Organopalladium Chemistry for Organic Synthesis*, Wiley, New York, 2002; (*d*) J. Hassan, M. Sevignon, C. Gozzi, E. Schulz and M. Lemaire, *Chem. Rev.*, 2002, **102**, 1359; (*e*) T. N. Mitchell, *Metal-catalyzed Cross-coupling Reactions*, Wiley-VCH, Weinheim, 2004; (*f*) A. C. Frisch and M. Beller, *Angew. Chem., Int. Ed.*, 2005, **44**, 674; (*g*) R. Martin and S. L. Buchwald, *J. Am. Chem. Soc.*, 2007, **129**, 3844; (*h*) M. Tobisu, T. Shimasaki and N. Chatani, *Angew. Chem., Int. Ed.*, 2008, **47**, 4866.

15 S. K. Kurtz and T. T. Perry, *J. Appl. Phys.*, 1968, **39**, 3798.